A&A 440, 367–371 (2005)
DOI: 10.1051/0004-6361:20053083

Astronomy & Astrophysics

What determines the radio polar brightening?

C. L. Selhorst[1], A. V. R. Silva[2], and J. E. R. Costa[1]

[1] CRAAM, Instituto Nacional de Pesquisas Espaciais, São José dos Campos, SP 12201-970, Brasil
e-mail: caius@craam.mackenzie.br
[2] CRAAM, Universidade Presbiteriana Mackenzie, São Paulo, SP 01302-907, Brasil

Received 17 March 2005 / Accepted 9 May 2005

Abstract. In order to explain the bright patches of emission near the poles of 17 GHz solar maps, we have applied a previously developed atmospheric model based on radio observations. This 2-D model, which includes spicules, yields results in good agreement with brightness temperature values at the disk center, radius, and limb brightening 17 GHz observations at equatorial and intermediate regions. Nevertheless, the intensity of discrete bright patches observed near the poles in 17 GHz maps (as bright as 40% over the quiet Sun), can only be explained by holes in the spicule forest. These regions without spicules probably reflect the presence of polar faculae, which inhibit the appearance of spicules. Moreover, the absence of spicules over faculae explains the anti-correlation between the mean polar limb brightening and the solar cycle, because the polar faculae are known be anti-correlated with the solar cycle. Results from the model with spicule-less regions showed that: 1) for bare regions of the same size (5°), the limb brightening increases with the pole proximity; 2) larger regions yield more intense limb brightening; 3) the average height of the spicules greatly influences the solar radius; 4) the maximum excess brightness temperature of 40% is in very good agreement with the polar limb observations above bright patches.

Key words. Sun: atmosphere – Sun: radio radiation – Sun: fundamental parameters – Sun: faculae, plages

1. Introduction

In operation since 1992, the Nobeyama Radioheliograph (NoRH, Nakajima et al. 1994) has provided an excellent data base to study solar features at 17 GHz. An example is the prominent limb brightening seen in the daily solar maps. Shibasaki (1998) showed that this polar brightening consisted of extended bright areas and patches that are about 40% more intense than the 17 GHz quiet Sun brightness. In Gelfreikh et al. (2002), the authors reported a spatial distribution of bright regions near the poles in 17 GHz maps that resemble polar faculae. Selhorst et al. (2003) showed the existence of an anti-correlation between the mean polar limb brightening and the solar cycle. Moreover, the overall limb brightening distribution is not uniform, with the relative mean intensities greater near the poles (25%) than in the equatorial (15%) or intermediate regions (10%).

In a previous work, Selhorst et al. (2005) developed an atmospheric model (hereafter referred to as the SSC model) in order to reproduce simultaneously three independent radio observations: the brightness temperature at disk center for frequencies ranging from 1.4 to 400 GHz, the observations of the radius and the limb brightening at 17 GHz. Moreover, the SSC is a 2-D model that takes into account the solar spherical curvature in order to study the solar radius and the limb brightening at 17 GHz. This model yields a radius of ~970″ at 1 AU which is about 5″ smaller than the mean observed value (Selhorst et al. 2004). As for the limb brightening, we obtained 36% of center-to-limb variation, which is compatible with the larger values detected at the solar poles. However, it is larger than the brightening observed at equatorial and intermediate regions (Selhorst et al. 2003).

Several authors have suggested that spicules were responsible for a decrease in the limb brightening observed at radio wavelengths (Elzner 1976; Fürst et al. 1974; Braun & Lindsey 1987). Thus, randomly distributed spicules were introduced in the SSC model. As a result of this heterogeneous atmosphere, the relative limb brightening was reduced to values of 12% above the quiet Sun. By varying randomly the physical parameters of spicules (such as density, temperature, height and inclination angle), the brightness temperature distribution across the disk agreed very well with observations at 17 GHz, except for the polar regions. Furthermore, the model has shown that the solar radius at 17 GHz is mainly determined by the average height of the spicules, increasing as the spicule height increases.

In this work, we discuss how the SSC model with spicules can describe the polar limb brightening at 17 GHz and the physical parameters involved in this solution. The next section summarizes the observations. In the third section we describe the SSC model with spicules and the implementation of regions without spicules. The comparison between the model and 17 GHz polar observations is presented in Sect. 4. Discussion

of the results and the main conclusions of this work are given in Sect. 5.

2. Observations

Daily solar maps from NoRH, with good spatial resolution (10–18″), from 1992 to 2004 were analyzed. This high spatial resolution enables the study of the limb brightening at 17 GHz, which has a large contribution from the bright patches observed near the poles, as can be seen in Fig. 1.

From the synthesized NoRH images, we have extracted the brightness temperature distribution profiles across the disk by taking radial scans that cross the center of the solar disk. Each cut provides a brightness temperature profile, where the brightening near the limb is quite evident, especially near the North Pole where the scan crosses a bright patch of emission (shown as a sharp increase on the right hand-side of the brightness profile in Fig. 1, bottom panel). The limb brightening has a nonuniform distribution as a function of latitude (Selhorst et al. 2003), with greater intensities at the poles mainly due to the presence of bright patches that reach brightness temperatures as high as 40% above the quiet Sun temperature. Because the polar brightening consists of many bright patches, frequently, the scan profiles may present different brightening in directly opposite limbs (as is the case of the profile shown in the bottom panel of Fig. 1).

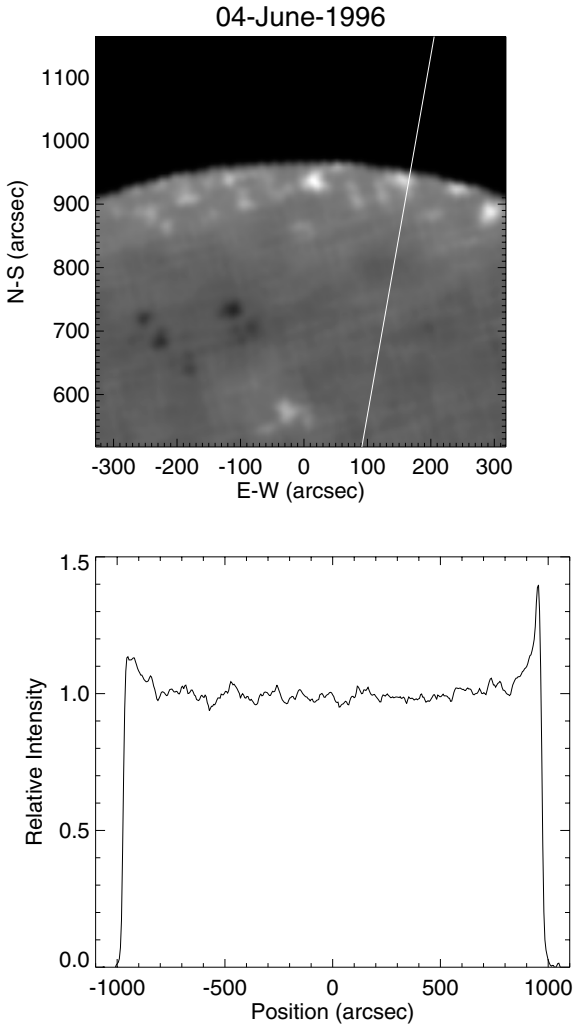

Fig. 1. *Top*: solar North pole of a 17 GHz map during the solar minimum. The white straight line represents a scan in the map, which yields the intensity profile shown in the bottom figure. The scan crosses a bright patch very close to the limb and the pole, that causes a sharp increase in the intensity profile near the limb.

3. 2-D atmospheric model with spicules

3.1. The SSC model

The atmospheric model previously developed (Selhorst et al. 2005) consists of temperature and density (electron and proton) distributions as a function of height, from the photosphere up to 40 000 km in the corona. The SSC model was developed as a bi-dimensional space reproducing one quadrant of the Sun. Two matrices were created representing the spatial distributions of temperature and the product of the electron and proton densities, $n_e n_p$. These matrices were divided into seven smaller matrices to facilitate computational handling, which were sequenced following the solar spherical curvature. The total angular region covered by the matrices is larger than one quadrant (90°), ranging from polar angles −10° through 100° to include the ray tracing at the limb.

To calculate the brightness temperature as a function of position across the solar disk, the emission mechanism at 17 GHz was assumed to be thermal bremsstrahlung. The radiative transport was calculated along paths represented by horizontal lines, separated by 1″ from each other. Thus, a brightness temperature profile from the center to the solar limb was obtained with an excess brightening of 100% near the limb. Assuming the Sun to be symmetric, this profile was folded around the Sun center. Since the NoRH maps have a maximum spatial resolution of 10″, the brightness temperature profile was convolved with a 10″ *FWHM* Gaussian beam. Then, the convolved excess temperature at the limb decreased to 36% above disk center values, which is very close to the maximum limb brightening observed in the polar region. However, it is still higher than the mean values observed in the equatorial (15%) and intermediate regions (10%).

To reduce even the further limb brightening and increase the solar radius at 17 GHz (in order to fit the observations) the presence of spicules were included. In the model, spicules are represented as cylinders of constant density and plasma temperature with typical spicule composition. The spicules were randomly distributed around the limb in the SSC model, inclined with respect to the solar surface replacing the temperatures and densities of the local atmosphere. This procedure resulted in a solar radius closer to the observational values and a limb brightening compatible with the brightening observed at equatorial and intermediate regions.

3.2. Model with spicule-less regions

As mentioned before,however, the solar maps at 17 GHz present limb brightening as high as 40% (Selhorst et al. 2003; Shibasaki 1998) above the quiet Sun values, that is

Table 1. Spicule-less simulation results.

Figure	Spicule parameter	Spicule-less region	Results			
	height	heliographic angle interval	center T_b	Limb bright.		radius
	(km)	(°)	(K)	(%)	width (″)	(″)
3a	5–7	76.2–81.4	10 720 ± 120	21.4	55.4	972.4
3b	5–7	78.5–83.7	10 670 ± 100	26.3	39.2	972.5
3c	5–7	80.2–85.5	10 700 ± 120	30.0	17.4	972.4
3d	5–7	80.2–90.0	10 740 ± 100	40.0	14.5	972.5
3e	5–10	80.2–90.0	10 800 ± 100	39.4	19.4	975.1

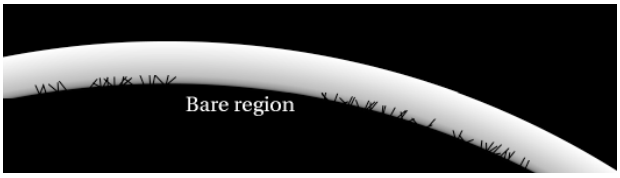

Fig. 2. Example of a bare region (region without spicules) near the pole, between 80 and 90°, in the temperature matrices.

not explained by the SSC model. Thus, a modification of the SSC model was needed in order to explain the 17 GHz emission near the poles. Therefore, we suggest that the discrete bright polar patches observed in 17 GHz maps are due to holes in the spicule forest right above polar faculae. Gaizauskas (1984) observed that there are no spicules over faculae as well as over plages (Zirin 1988). Moreover, faculae are known to be more abundant near the poles (Erofeev 2001; Unruh et al. 1999; Ortiz et al. 2002) and the radio polar bright regions are close to the polar faculae regions (Riehokainen et al. 1998; Gelfreikh et al. 2002).

To test this hypothesis, model simulations were performed with regions without spicules near the poles (Fig. 2). In all simulations, the spicules were 500 km wide, random temperatures from 7 to 13×10^3 K, electron and ion densities ranging from 2 to 6×10^{10} cm^{-3}, and randomized inclination angles from 30 to 150° (Sterling 2000; Zirin 1988, and references therein). The results of the simulations are listed in Table 1 and plotted in Fig. 3, each result represents a mean of 20–40 simulations with all spicules randomly generated around the limb. The first column shows the figure panel related to the simulations, the second column shows the height range of the spicules, and the heliographic angles of regions without spicules in the simulations are shown in the next column. The results are listed in the next four columns: the model brightness temperature at disk center, the limb brightening intensity and its width, and the resultant solar radius.

The first three simulations presented in Table 1 (a–c) have regions without spicules within a 5° heliographic interval. However, the distances of these regions to the pole are different. These simulations show a higher limb brightening for spicule-less regions closer to the pole, whereas the limb brightening width decreases due to projection effects of the solar curvature. For example, the limb brightening intensity increases from 21.4 to 30.0% as the bare region approaches the pole (first and third simulations), whereas the width shows a larger abrupt decrease

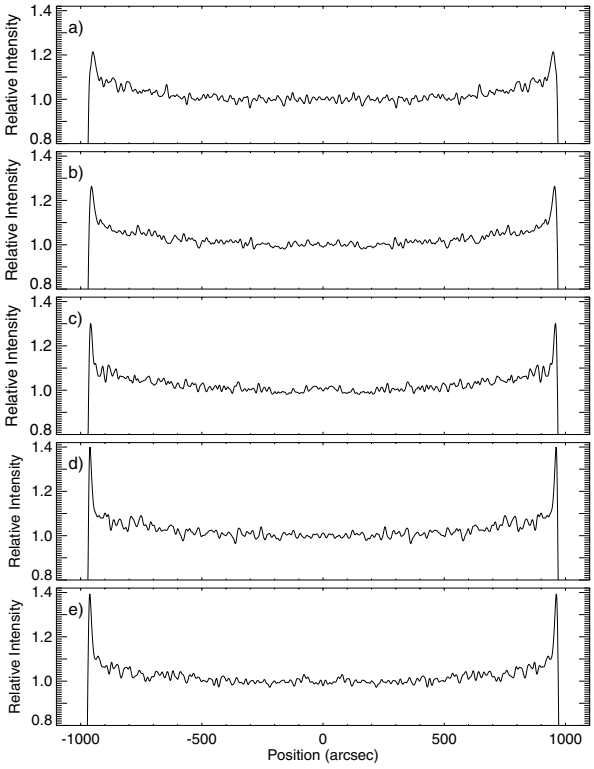

Fig. 3. Center-to-limb brightness temperature profile, calculated as the mean of a set of simulations using the SSC atmospheric model with regions without spicules. Each panel represents a bare region with different parameters, which are listed in Table 1.

from 55.4 to 17.4″ in the same simulations. The increase in the max intensity of the limb brightening accompanied by a decrease in its width is clearly seen in the top three panels of Fig. 3.

In the last two simulations, the role of the spicule height was studied in the simulations with a spicule-less region. In these simulations, the area of the region without spicules was twice as large as those in the first three models of Table 1. The results show a thin and intense limb brightening, that reached approximately 40% above the quiet Sun values in both simulations (Figs. 3d and 3e). These limb brightening values are larger than those obtained from the SSC model without spicules (36%, see Selhorst et al. 2005). This result can be explained by spicules located beyond 90°, which are optically thick and emit more at 17 GHz than the replaced local atmosphere.

The very narrow limb brightening width is explained by the location of the bare region, between 80.2–90.0°. At this location the projected area is only about 15″, which would be the apparent size of a bright region on a solar map. Moreover, the results yield a radius increase, which implies that the spicule height is more important for a radius increment than for limb brightening.

4. Comparison between the model and the 17 GHz polar observations

The polar limb brightening observed at 17 GHz is not homogeneous (Selhorst et al. 2003), moreover the observations show the existence of compact bright patches unevenly distributed around the limb. In this section we present the results of a comparison between the observations and simulations. The observation considered here is a scan close to the solar poles of a 17 GHz solar map taken during the last solar minimum (June 4th, 1996). The scan crosses an intense bright patch in the North pole (Fig. 1), while the other pole presents the usual limb brightening of approximately 13% (Fig. 4, gray curve). The scan intensity was normalized to the quiet Sun brightness temperature (taken as the most common value of the map).

First, the brightness temperature calculated from the SSC model was obtained by varying randomly all physical parameters of the spicules (except the width which was fixed at 500 km) which were distributed randomly throughout the limb. The spicules physical parameters were randomly chosen from ranges in temperatures (7000–13 000 K), densities (2–6 $\times$ 10^{10} cm^{-3}), inclination angle (30°–150°) and heights (5000–7000 km). The result for this simulation (Fig. 4a black line) was 14% of limb brightening that matches the observation of the Southern pole (left hand-side of Fig. 4a).

Nevertheless, to reproduce the 40% limb brightening intensity observed in the Northern pole, a bare region from 80.2 to 90.0° heliocentric angles was included in the simulation. The physical parameters of the spicules outside this region were the same as in the previous simulation. The resulting brightness profile, taken as a mean of 27 simulations, the same as in Fig. 3d and Table 1, is shown as a dark solid line on the right of Fig. 4b. As can be seen from the figure, the model with a bare region represents very well the observed limb intensity (40% above the quiet Sun), however, the limb brightening width is narrower than the observed one. A modification in the temperature distribution above this spicule-less region could increase this width.

5. Discussion and conclusions

The SSC atmospheric model developed by Selhorst et al. (2005) showed that spicules distributed randomly throughout the limb reduce the simulated limb brightening at 17 GHz to values close to the mean values observed in equatorial (15%) and intermediate regions (10%). Nevertheless, there are discrete bright patches that can reach up to 40% above the quiet Sun brightness temperature, especially near the polar limb. It is known that there are no spicules over chromospheric plages (Shibata & Suematsu 1982; Zirin 1988) and the same behavior

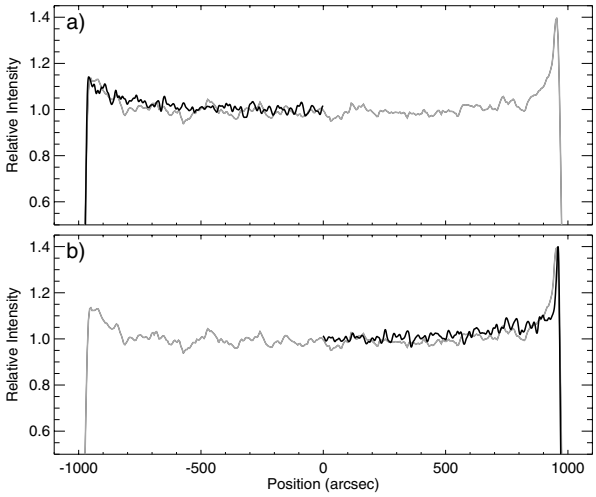

Fig. 4. Comparison between the observed 17 GHz brightness temperature profile (gray curve) and **a)** the mean of SSC model simulations with spicules distributed throughout the limb and **b)** with spicule-less regions close to the North pole.

was observed for faculae (Gaizauskas 1984). Moreover, polar faculae and polar limb brightening are both anti-correlated with the sunspot cycle (Efanov et al. 1980; Makarov & Makarova 1996; Koshiishi 1996; Selhorst et al. 2003). Therefore, based on these observations, we suggest that holes in the spicule forest associated with faculae could yield patches of intense limb brightening near the solar poles.

To test this hypothesis, we have performed simulations containing regions without spicules near the poles at different positions and for 2 distinct sizes. These simulations with spicule-less regions have shown that:

1. for regions of 5° in size, the limb brightening increases with the pole proximity;
2. larger region result in more intense limb brightening;
3. the average height of the spicules influences more the solar radius than the maximum of the limb brightening at 17 GHz;
4. the maximum excess brightness temperature obtained was 40%, in very good agreement with the polar limb observations above bright patches.

Although the presence of spicules reduces the limb brightening at 17 GHz to values close to those observed in solar equatorial and intermediate regions, the existence of small regions without spicules could produce intense patches of radio emission near the solar poles. These polar bare regions are probably associated with the presence of faculae in these region.

The model proposed here considers only the bremsstrahlung emission, which for distinct radio frequencies is produced in different heights of the solar atmosphere. The presence of spicules in the atmosphere changes the local physical parameters, such as temperatures and densities (electrons and ions), yielding different values for the brightness temperature. Thus, the resulting limb brightening will vary according to the radio wavelength. For example, at higher frequencies, the brightening at the solar limb could be reduced or even completely suppressed.

To improve the model, changes in the local atmosphere (temperature and densities) caused by the presence of faculae should be made in order to provide a better agreement with observations.

Acknowledgements. We are grateful to the NoRH staff for obtaining the full disk 17 GHz maps and making them available over the Internet. The Nobeyama Radioheliograph is operated by NAOJ/Nobeyama Solar Radio Observatory. C.L.S. acknowledges financial support from the Brazilian agency FAPESP, grant number 01/02106-3.

References

Braun, D., & Lindsey, C. 1987, ApJ, 320, 898
Efanov, V. A., Moiseev, I. G., Nesterov, N. S., & Stewart, R. T. 1980, in Radio Physics of the Sun, IAU Symp., 86, 141
Elzner, L. R. 1976, A&A, 47, 9
Erofeev, D. V. 2001, Sol. Phys., 203, 9
Fürst, E., Hachenberg, O., & Hirth, W. 1974, A&A, 36, 123
Gaizauskas, V. 1984, Sol. Phys., 93, 257
Gelfreikh, G. B., Makarov, V. I., Tlatov, A. G., Riehokainen, A., & Shibasaki, K. 2002, A&A, 389, 618
Koshiishi, H. 1996, Ph.D. Thesis
Makarov, V. I., & Makarova, V. V. 1996, Sol. Phys., 163, 267
Nakajima, H., Nishio, M., Enome, S., et al. 1994, Proc. IEEE, 82, 705
Ortiz, A., Solanki, S. K., Domingo, V., Fligge, M., & Sanahuja, B. 2002, A&A, 388, 1036
Riehokainen, A., Urpo, S., & Valtaoja, E. 1998, A&A, 333, 741
Selhorst, C. L., Silva, A. V. R., & Costa, J. E. R. 2004, A&A, 420, 1117
Selhorst, C. L., Silva, A. V. R., & Costa, J. E. R. 2005, A&A, 433, 365
Selhorst, C. L., Silva, A. V. R., Costa, J. E. R., & Shibasaki, K. 2003, A&A, 401, 1143
Shibasaki, K. 1998, in ASP Conf. Ser., 140, 373
Shibata, K., & Suematsu, Y. 1982, Sol. Phys., 78, 333
Sterling, A. C. 2000, Sol. Phys., 196, 79
Unruh, Y. C., Solanki, S. K., & Fligge, M. 1999, A&A, 345, 635
Zirin, H. 1988 (New York, EUA: Cambridge University Press)